Eur. Phys. J. D **7**, 323–330 (1999)

THE EUROPEAN PHYSICAL JOURNAL D

EDP Sciences

Differential measurement of the ultracold Cs radiative escape and fine structure changing collision rates

J.P. Shaffer, W. Chalupczak, and N.P. Bigelow[a]

Department of Physics and Astronomy, Laboratory for Laser Energetics, University of Rochester, Rochester, New York 14627, USA

Received 4 December 1998 and Received in final form 18 March 1999

Abstract. We present direct measurements of the overall trap loss rate and the fine structure changing collision rate for ultracold cesium atom confined in a magneto-optical trap over an intensity range of 5 mW/cm^2 to 200 mW/cm^2. This set of simultaneous measurements allows the accurate extraction and separation of the fine structure changing rate and the radiative escape rate as these two processes compete with one another to determine the overall trap loss rate.

PACS. 32.80.Pj Optical cooling of atoms; trapping – 34.50.Rk Laser-modified scattering and reactions

1 Introduction

The development of laser cooling and trapping techniques has provided a means to explore collisional physics in an entirely new regime. The magneto-optical trap (MOT) allows the experimentalist to generate samples of atoms at submilli-kelvin temperatures and densities of $> 10^{10}$ cm^{-3}. Collisions between these laser cooled and trapped atoms have a number of unique properties such as their sensitivity to the long range interatomic potentials and their basic quantum nature. Perhaps, though, the most interesting property of ultracold collisions is that the duration of these events can be longer than the spontaneous emission time scale. Because the decay time may be shorter than the duration of an ultracold collision, spontaneous emission during a collision can result in trap loss as kinetic energy is transferred to the colliding atoms from the electromagnetic field. Such processes are among the dominant loss mechanisms in the MOT and are referred to as radiative escape (RE).

Because alkali atoms are relatively easily cooled and trapped in a MOT, many studies of trap loss in these types of traps have been carried out. Trap loss has been studied in Li [1], Na [2], Rb [3], and Cs [4]. These investigations have addressed many questions such as the roles of hyperfine structure [5], the long range part of the collision [6], and re-excitation [7].

One problem with the experimental investigation of trap loss in the MOT is that it is difficult to separate out the different types of collisional processes. Few studies have been able to separate the fine structure (FS) collision loss from that due to RE. In the special case of Li, it was possible to infer the RE collision rate from the overall trap loss data because the fine structure splitting in Li is less than the trap depth for commonly achievable trapping parameters [1], thus eliminating the FS loss channel. In a related experiment, the loss rate from a Na trap which was run on the D1 line, and which is thus immune to FS loss processes, was measured [8]. Perhaps the most conclusive results concern Cs, where the presence of FS changing collisions was elegantly demonstrated by direct observation of D1 line photons emitted by the atoms during the collision [9]. In the present paper we present the results of a simultaneous measurement of the intensity dependent overall trap loss rate and the FS changing collision rate for Cs atoms in a MOT. Our results are in excellent agreement with previous studies yet represent a distinct advancement in that in our work both trap loss and FS loss rates are studied in the same physical trap set-up, under identical conditions including trapping laser parameters, beam profiles, chamber background pressures, etc. As a result, our measurements allow us to separate the FS changing collisions from the RE collisions with significant confidence and to provide new insight into the interplay of the various trap loss processes of the MOT.

Two distinct trap loss processes which occur between a ground and an excited state ultracold trapped atom have been identified in homonuclear alkali traps [10]. Both of these processes happen when a pair of ground state atoms approach each other and absorb a trapping laser photon at long range ($\sim$ 800 Å). At this point, the ground state interatomic potential energy ($\sim C_6/R^6$-essentially flat) and the excited state interatomic potential energy ($\sim C_3/R^3$) resulting from an attractive resonant dipole-dipole interaction, bring the colliding pair into resonance with the trapping fields. A trap photon can be absorbed at or near the point of resonance and a molecule is created by photoassociation. Both of the most significant trap loss

[a] e-mail: nbig@lle.rochester.edu

processes in a homonuclear trap begin in this way because of the large cross-section for absorption at long range due to the long range resonant dipole interaction.

Because the atoms in the MOT are cold, there is a significant chance that as the atoms accelerate towards one another on an attractive potential the complex will radiate and transfer kinetic energy to the atomic pair. If this energy is greater than twice the trap depth, the now hot atoms will escape from the trap. This process is called radiative escape (RE) and is represented in the case of Cs by,

$$\mathrm{Cs}(6^2\mathrm{S}_{1/2}) + \mathrm{Cs}(^2\mathrm{S}_{1/2}) + \hbar\omega_{\mathrm{trap}} \rightarrow \mathrm{Cs}_2^*(6^2\mathrm{S}_{1/2} + 6^2\mathrm{P}_{3/2}) \rightarrow \mathrm{Cs}(6^2\mathrm{S}_{1/2}) + \mathrm{Cs}(6^2\mathrm{S}_{1/2}) + \Delta\varepsilon_{\mathrm{RE}} + \hbar\omega_{\mathrm{emitted}} \quad (1)$$

where $\Delta\varepsilon_{\mathrm{RE}} = \hbar(\omega_{\mathrm{trap}} - \omega_{\mathrm{emitted}})$.

The second process which may occur is that the photoassociated complex may undergo a change of fine structure at long range induced by the resonant dipole interaction or at close range in the region of exchange interactions. The long range mechanism is particularly strong in the lighter alkalis such as Na. The couplings at close range may be due to heterogeneous interactions (Coriolis effects – S uncoupling which causes the transition from Hund's case (a) to (b) coupling) or rotational mixing at radii where Hund's case (c) to case (a) coupling occurs (spin-orbit mixing) [11,12]. If half the fine structure splitting, $\Delta\varepsilon_{\mathrm{FS}}$, of the trapped atoms is larger than the trap depth the colliding pair will escape the trap. In general $\Delta\varepsilon_{\mathrm{FS}}$ is large enough for all the atoms undergoing these types of collisions to escape the trap. This is certainly true in the case of Cs where $\Delta\varepsilon_{\mathrm{FS}} = 554\ \mathrm{cm}^{-1}$. These processes are generally referred to as FS changing collisions and are represented in the case of Cs by,

$$\mathrm{Cs}(6^2\mathrm{S}_{1/2}) + \mathrm{Cs}(6^2\mathrm{S}_{1/2}) + \hbar\omega_{\mathrm{trap}}(852\ \mathrm{nm}) \rightarrow \mathrm{Cs}_2^*(6^2\mathrm{S}_{1/2} + 6^2\mathrm{P}_{3/2}) \rightarrow \mathrm{Cs}_2^*(6^2\mathrm{S}_{1/2} + 6^2\mathrm{P}_{1/2}) \rightarrow \mathrm{Cs}(6^2\mathrm{S}_{1/2}) + \mathrm{Cs}(6^2\mathrm{S}_{1/2}) + \Delta\varepsilon_{\mathrm{FS}} + \hbar\omega_{\mathrm{P1/2}}(894\ \mathrm{nm}). \quad (2)$$

In this work we deduce the ratio of RE and FS loss rates for an ultracold sample of Cs in a MOT. We directly measure the FS ultracold collision rate as a function of the trapping laser intensity, building on the work of [9] and in addition, we provide a simultaneous, new and accurate measurement of the Cs trap loss rate also as a function of trapping laser intensity. With these two measurements we are able to extract the RE ultracold collision rate for Cs. We find that the RE rate reaches a constant value. Our observations differ from previous predictions where the RE rate was thought to decrease as the trap depth increased [13]. Finally, we provide a cross-section for RE given that the sample temperature is approximately equal to the Doppler temperature, $T_{\mathrm{Doppler}} = \hbar\Gamma_{\mathrm{Cs}}/2k_{\mathrm{B}} = 144\ \mu\mathrm{K}$ for intensities, $I \gg I_{\mathrm{sat}} = 1.06\ \mathrm{mW/cm}^2$.

2 Experiment

The experiment is run in the standard MOT configuration [14]. The chamber is run with a background pressure $\leq 10^{-10}$ torr and a magnetic field gradient of 20 gauss/cm. The trap is loaded from an uncooled source [15]. The optical fields are generated by a stabilized ring dye laser running at ~ 852 nm. The trapping laser is run with a linewidth ~ 1 MHz and is referenced by saturated absorption spectroscopy to the Cs atomic spectrum. The Cs trap laser is red detuned by $\Delta = -4.4\Gamma$, from the Cs $6^2\mathrm{S}_{1/2}(F=4) \rightarrow 6^2\mathrm{P}_{3/2}(F'=5)$ transition. A diode laser repumps the Cs $6^2\mathrm{S}_{1/2}(F=3) \rightarrow 6^2\mathrm{P}_{3/2}(F'=4)$ transition. Throughout the experiment the Cs repumping light had a constant intensity of 1.4 $\mathrm{mW/cm}^2$. The trapping light passes through a single mode optical fiber which spatially filters the light before it enters the trap. Trap beam profiles and alignments were therefore highly reproducible and independent of laser detuning and intensity. The trapping beams travel throughout the apparatus with diameters ~ 25 mm. The trapping beam intensities are continuously variable throughout the range 5–300 $\mathrm{mW/cm}^2$. The trap densities and number of atoms may be found in [16]. For most of the range of the experiment the density was $\sim 10^{10}\ \mathrm{cm}^{-3}$.

The volume of the trap was measured as a function of intensity and time during the filling of the trap. We find that when the MOT laser beams were carefully aligned the traps are consistently oblate spheroids in shape with an eccentricity $= \sqrt{2}/2$ reflecting the shape of the magnetic field (the field gradient along the axis of the anti-Helmholtz coils is twice that found along the radius of the coils). We therefore choose to characterize the traps by a single radius. This radius was measured and verified by acquiring an image of the trap with two CCD cameras. A Gaussian profile was then fit to the trap cloud image to determine the full width at half maximum, σ. We found that a Gaussian shape fit the trap cloud image well throughout the entire range of our experiment [16].

The number of trapped atoms was measured through the fluorescence signal detected by a photomultiplier tube (PMT). The PMT was calibrated at 852 nm with light from the Cs trapping laser and all frequencies were tuned by saturated absorption spectroscopy. The fluorescence was converted into the number of trapped atoms, N, using $N = R_{\mathrm{fl}}/\Gamma_{\mathrm{Cs}}\Theta\rho_{\mathrm{ee}}$, where Γ_{Cs} is the spontaneous decay rate for the trapping transition ($\Gamma_{\mathrm{Cs}} = 6$ MHz), R_{fl} is the fluorescence rate detected by the PMT, ρ_{ee} is the excited state population and Θ is a geometrical factor determined by the angle subtended by the detector with respect to the trap cloud. ρ_{ee} is determined with a six level two field steady state calculation [17] where one field was the repumping field, the other field was the trapping field, and the six levels correspond to the hyperfine structure of the Cs $6^2\mathrm{S}_{1/2} \rightarrow 6^2\mathrm{P}_{3/2}$ transition. The populations deduced in this way were in excellent agreement with experimental measurements [9].

The trap loss rate is determined by monitoring the fluorescence of the atoms as they fill the MOT. The rate

equation for this process can be written as,

$$\frac{\mathrm{d}N_i(t)}{\mathrm{d}t} = L - \alpha N_i(t) - \frac{\beta}{V} N_i^2(t). \tag{3}$$

This is in the form of a Ricatti equation with constant coefficients. L is the trap loading rate, α is the loss rate due to collisions between ultracold trapped atoms and background atoms and β is the loss rate due to collisions between ultracold trapped atoms. Our equation may be solved explicitly using the transformation; $N_i(t) = V/\beta[(\mathrm{d}N_i(t)/\mathrm{d}t)/N_i(t)]$, where we have assumed V is a constant. If the trap is initially empty the solution is

$$N_i(t) = \frac{2L\sinh[\gamma t/2]}{\alpha\sinh[\gamma t/2] + \gamma\cosh[\gamma t/2]} \tag{4}$$

where $\gamma = \sqrt{\alpha^2 + 4L\beta/V}$. This expression was used to calculate the trap loss rate constant from the time dependent fluorescence rate of atoms during filling of the MOT. As $t \to \infty$ the steady state number of atoms in the trap is, $N_\infty = \lim_{t\to\infty} N_i(t) = 2L/(\alpha + \gamma)$. This expression reflects the fact that the number of atoms in the trap is limited by a balance between collisions and the loading rate of the trap. If $\sqrt{4L\beta/V} \gg \alpha$ the number of atoms in the MOT is ultimately limited by rates of collisions between ultracold trapped atoms and

$$N_i''(t) = \sqrt{\frac{LV}{\beta}}\tanh\left(\frac{\gamma}{2}t\right) \tag{5}$$

with $N_\infty'' \approx \sqrt{LV/\beta}$.

To justify the assumption that $\sqrt{4L\beta/V} \gg \alpha$, we: (1) note that for similar chamber pressures and trapped atom densities, other workers have shown the trap losses to be dominated by two-body collisions [3,4] and (2) estimate α [18] as $\alpha \approx (1/4)\pi\sigma_{\mathrm{FS}}\overline{v}\rho_{\mathrm{back}}\rho_{\mathrm{ee}}$. Since the FS contribution to Cs trap loss is believed to be comparable to other contributions [9], for our estimate of α we use the known value of σ_{FS} which for Cs is $\sigma_{\mathrm{FS}} = 3.1 \times 10^{-15}$ cm^2 [11,19]. For a background, ρ_{back}, density of 10^6 cm^{-3} ($\sim 10^{-10}$ torr) and $\overline{v} = (v_{\mathrm{rms}})_{\mathrm{Cs}} = 389$ m/s with the laser intensity above saturation, $\alpha_{\mathrm{Cs}} \sim 0.001$ Hz [20]. Since $\sqrt{4L\beta/V} \approx 10^{-1}$–1 Hz and $\alpha \approx 10^{-3}$ Hz at a background pressure of 10^{-10} torr the approximation $\sqrt{4L\beta/V} \gg \alpha$ is well-satisfied. These values compare well with our collision rate measurements and are in good agreement with those of others [4].

The direct measurement of the fine structure collision rate for Cs is made by detecting D1 light emission from the trapped sample. This is done by collimating the trap fluorescence and sending this light through a 10 nm bandwidth filter centered around the $6S_{1/2} \to 6P_{1/2}$ (894 nm) transition of Cs. After the light from the trap is passed through the interference filter it is imaged through a SPEX 1700-2 1m monochromator adjusted for an 8 Å bandpass. This is necessary to filter out photons from the wing of the $6^2S_{1/2} \to 6^2P_{3/2}$ (852 nm) trapping transition. The inset of Figure 4 shows the bandpass of the

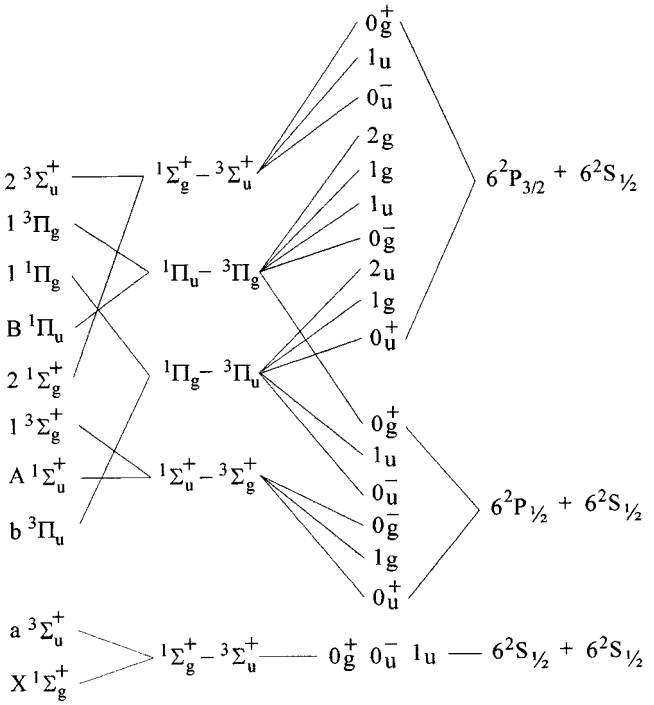

Fig. 1. The correlation diagram for Cs_2. The right hand side of the diagram shows the separated atom states relevant to the MOT. The cooling transition is $6^2S_{1/2} \to 6^2P_{3/2}$. From left to right the internuclear separation increases. On the left hand side of the diagram are separated Hund's case (a) states. Immediately to the right of these states are the intermediate Hund's case (a) states where the spin-orbit interaction has not yet separated the case (a) states. At still further internuclear separations are the Hund's case (c) states. The attractive states which contribute to ultracold collisions are 1_u, 0_g^-, 2_u, 1_g, and 0_u^+ all of which correlate with the singly excited Π states.

monochromator and demonstrates that the fluorescence from the $6^2P_{3/2} \to 6^2S_{1/2}$ trapping transition has successfully been filtered out of the $6^2P_{1/2} \to 6^2S_{1/2}$ fluorescence signal. The photons passing through the system are detected by an avalanche photodiode (APD) (dark counts < 100 Hz). The quantum efficiency of the APD was calibrated at 894 nm by the manufacturer (EG&G) and the APD was also cross-calibrated against the PMT used to detect the fluorescence from the trap. This was accomplished by using light from the Cs trapping laser tuned to the $3^2S_{1/2} \to 3^2P_{1/2}$ transition of atomic Cs. The fact that the laser was indeed at 894 nm was verified by saturated absorption spectroscopy. The product of the measured monochromator throughput and the quantum efficiency of the detector was 0.104 and the measured transmission including geometrical through the imaging system was measured to be 2.6×10^{-3}. The loss through the imaging system and monochromator was measured by passing light generated by the Cs trapping laser, again tuned by saturated absorption spectroscopy to either 852 or 894 nm, through the entire fluorescence collection/detection system, following the *exact path* of the trap fluorescence. The filter transmission coefficient was measured to be 3.52×10^{-7} at 852 nm and 0.500 at 894 nm.

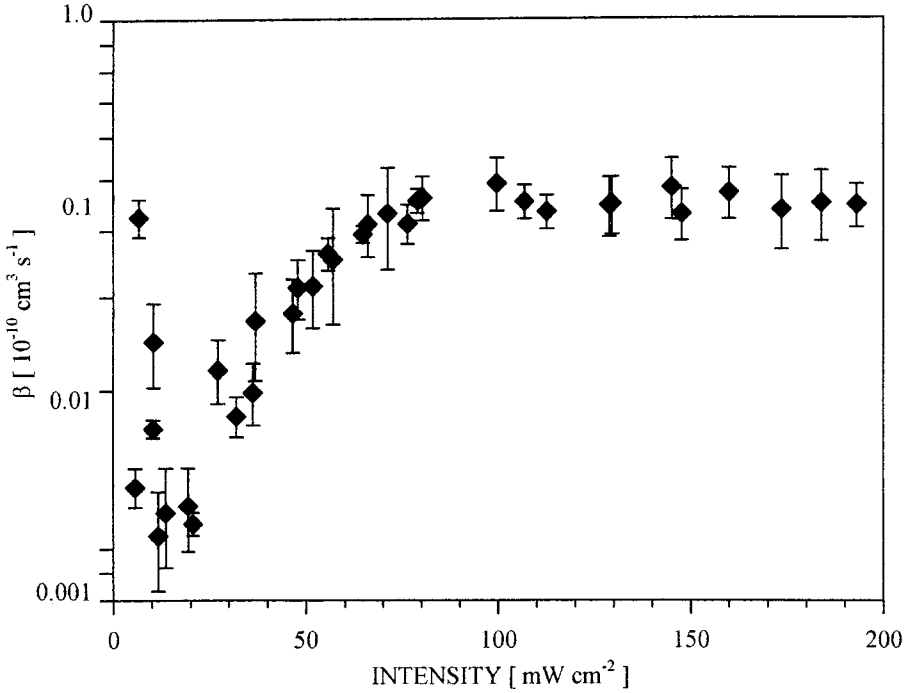

Fig. 2. The trap loss rate β as a function of laser intensity for a detuning of $\Delta = -4.4\Gamma$. The error bars reflect the mean squared fluctuation of the experiment. Each point is the average of approximately 20–30 measurements.

The filter attenuation at 894 nm was measured (1) using the Cs trapping laser and (2) using a calibrated spectrophotometer. The transmission losses of the vacuum chamber windows were independently verified using the Cs trapping laser as the light source at both 894 nm and 852 nm. In our experiments the maximum FS photon count rates were approximately 40 Hz.

3 Discussion

Figure 1 shows the correlation diagram for the molecular levels of Cs_2 for the states relevant to collisions which occur in the MOT. The hyperfine structure is not shown. The attractive long range Hund's case (c) levels are 1_u and 0_g^- which correlate to the $^1\Pi_u - ^3\Pi_g$ Hund's case (a) states ($6^2S_{1/2} + 6^2P_{3/2}$ asymptote) and 2_u, 1_g, and 0_u^+ which correlate to the $^1\Pi_u - ^3\Pi_g$ Hund's case (a) states ($6^2S_{1/2}+6^2P_{3/2}$ asymptote). According to this correlation diagram the only exoergic process which can occur when two atoms collide is a collision which results in a change of fine structure. Changes of hyperfine structure may cause trap loss as well but the energy separation between the $6^2S_{1/2}(F = 4)$ and the $6^2S_{1/2}(F = 3)$ ground state hyperfine levels is ~ 9.1 GHz which is less than the trap depth for total intensities above ~ 20 mW/cm^2. The fact that in the high intensity regime there are only two significant processes (RE and FS) one of which may be measured directly (FS changing collisions [9]) supports our argument that by accurately measuring the overall trap loss rate and the FS changing collision rate *simultaneously* we may extract the loss rate due to RE. This is a familiar example of a differential measurement which can be used to separate the two dominant channels of trap loss.

Figure 2 shows the measured trap loss rate for the Cs trap as a function of trapping laser intensity for a fixed detuning of $\Delta = -4.4\Gamma$. The rates at low intensity are in good agreement with previous work [4]. The shape of the curve has been discussed in the literature and is due to the different types of trap loss processes which occur and their interplay with the trap depth and atom recapture processes. The trap depth in units of energy for a one-dimensional Doppler model [16,21] is shown in Figure 3. In this light, consider Figure 2. Initially, as the intensity of the trapping light increases the trap loss rate decreases. The reason for this is that as the intensity is increasing the trap depth is increasing as well. This process attenuates the losses due to hyperfine changing collisions. The trap loss rate reaches a minimum at around 20 mW/cm^2. This value of intensity corresponds to a trap recapture energy of ~ 4.6 GHz which is approximately one-half of the ground state hyperfine splitting of Cs (9.1 GHz). As the intensity of the trapping beams increases still further, the excited state fraction in the sample increases and the processes of RE and FS become dominant. This is exhibited in the increase in trap loss rate above 20 mW/cm^2. The fact that this rate increases linearly with intensity until it saturates is in agreement with a weak field assumption [12,22].

Figure 4 shows the FS collision rate measured directly by observing 894 nm photons emitted from the Cs MOT. In a similar fashion to that observed in Figure 2, the FS rate increases sharply as the intensity grows for $I > 20$ mW/cm^2. The rate when $I \gg I_{\rm sat}$ is $\beta_{\rm FS} = 1.8 \times 10^{-11}$ cm^3/s for $\Delta = -4.4\Gamma$.

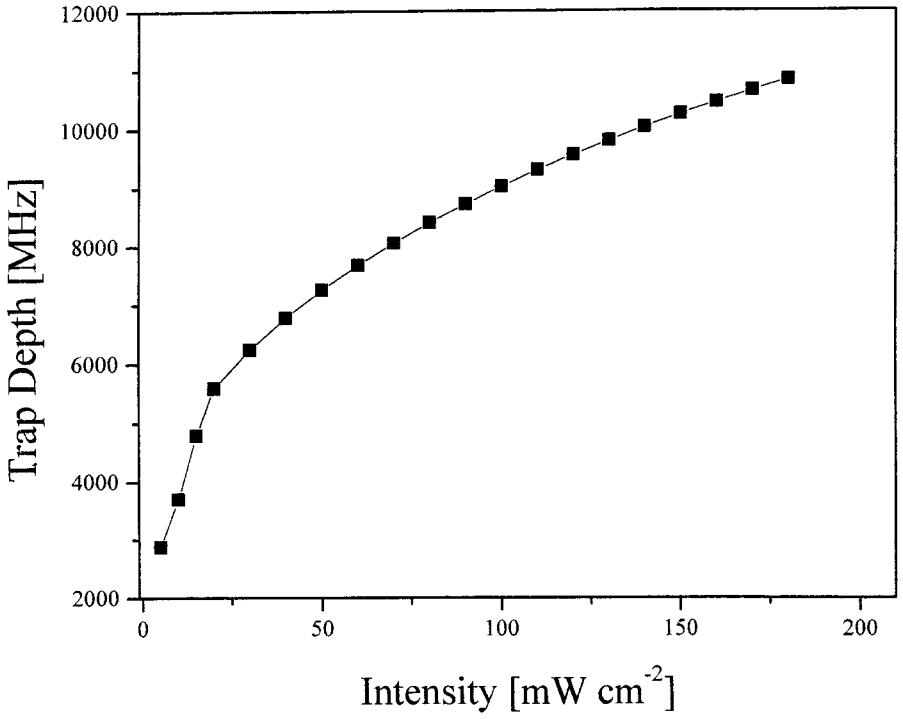

Fig. 3. The trap depth as a function of intensity. The values on this particular curve were calculated as $1.5mv_{\rm crit}^2$ where $v_{\rm crit}$ is the capture velocity of the Cs MOT for a 1 dimensional Doppler model. For more details about this calculation see [15,20]. The parameters used were those used in the experiment and may be found in the text.

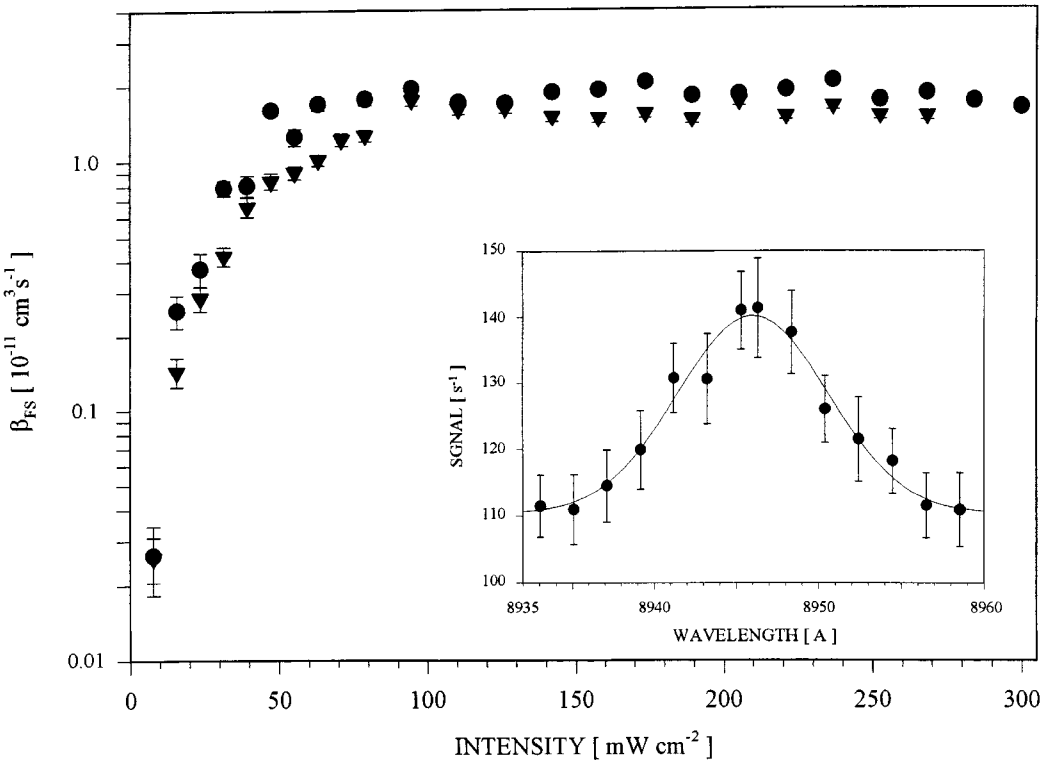

Fig. 4. The FS changing collision trap loss rate $\beta_{\rm FS}$ as a function of intensity for a detuning of $\Delta = -4.4\Gamma$. The error bars reflect the mean squared fluctuation of the experiment. Each point is the average of approximately 100 measurements. The inset shows the measured bandpass of the monochromator.

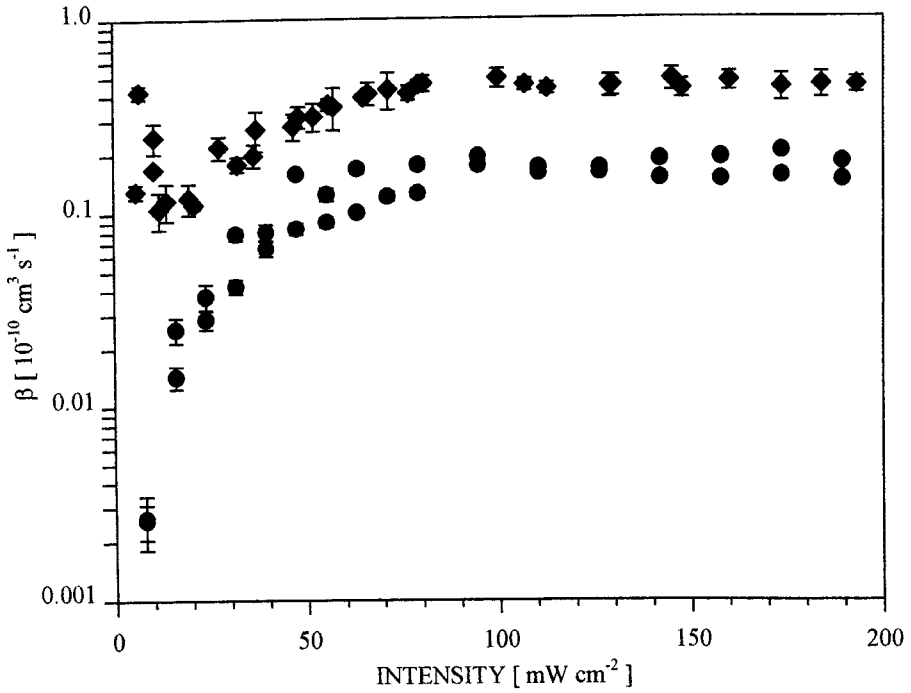

(a)

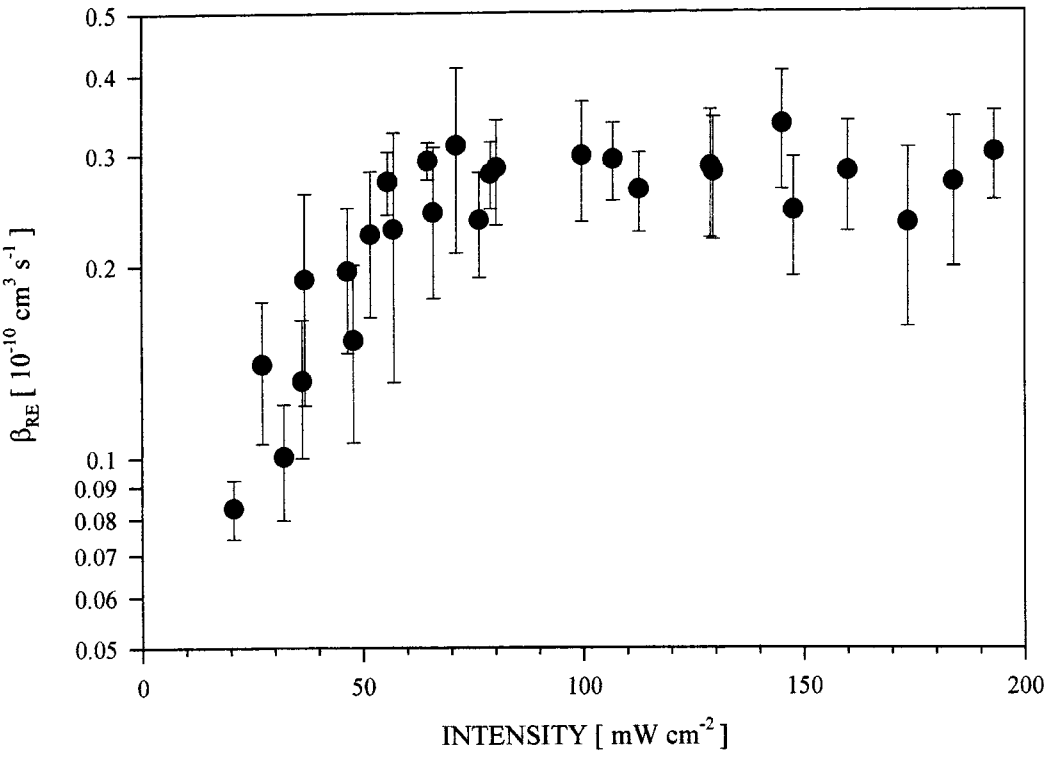

(b)

Fig. 5. (a) Plot which shows the relative relationship between β_{FS} and β_{RE}. The data is the same as that found in Figures 2 and 4. (b) The radiative escape rate $\beta_{\mathrm{RE}} = \beta - \beta_{\mathrm{FS}}$ for a detuning of $\Delta = -4.4\Gamma$. The error bars are the mean squared average of the β error and the β_{FS} error.

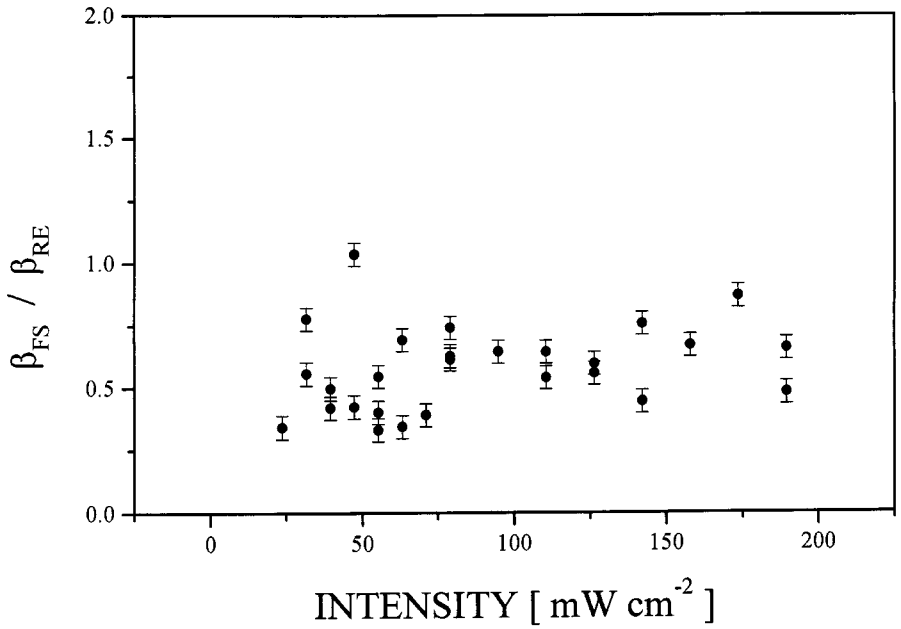

Fig. 6. The ratio $\beta_{\rm FS}/\beta_{\rm RE}$ for a detuning of $\Delta = -4.4\Gamma$. The scatter in the plot gives a measure of the uncertainty in this value. The data points were fit to a constant to establish that $\beta_{\rm FS}/\beta_{\rm RE} = 0.58 \mp 0.03$.

The intensity dependence of $\beta_{\rm FS}$ and the saturated absolute value of $\beta_{\rm FS}$ agree well with the value 1.1×10^{-11} cm^3/s measured at a detuning of $\Delta = -3\Gamma$ as presented in [9]. Given the atom temperature ($\sim 144\ \mu$K) (at high; $I > 50$ mW/cm^2) our rate corresponds to a cross-section of $\sigma_{\rm FS}(I > 50\ {\rm mW/cm^2}) = 1.1 \times 10^{-13}$ cm^2. We note that the cross-section is 22 times larger than the high temperature result [11,19]. This indicates that, as pointed out by Julienne and Vigué [12], the cross-section for FS changing collisions indeed does not simply scale as the thermal wavelength.

To understand this scaling, we note that the probability of a change of FS during a collision is temperature dependent at high temperatures, whereas the rate is dominated by the accessible angular momentum at low temperatures. In fact, at the microKelvin temperatures characteristic of the MOT, the limited amount of angular momentum (a limited number of partial waves – "l" values) determines to the FS cross-section. One consequence is that the crossing probability (the probability to undergo a change of FS) at the potential curve crossing, in a Landau-Zener picture, becomes almost temperature independent at low energies (for fixed angular momentum) since the velocity spread of the atoms is small compared to the energy splitting at the crossing point.

We also note that Julienne and Vigué have calculated the FS rate for different input channels and they find that for Cs the 0_u^+ input channel contributes almost exclusively to the FS changing collision loss rate [12]. Although we did not explore the resulting role of hyperfine structure on the rate of FS changing collision rate, we note that this was a primary focus of the complementary work of the Pisa group [9]. Figure 5b shows the RE collision rate as a function of intensity. Figure 5a illustrates the relative size of the total trap loss, β, as compared to the loss due to FS changing collisions, $\beta_{\rm FS}$. The points in Figure 5b were calculated by subtracting $\beta_{\rm FS}$ from β. The rate of RE type collisions is then, $\beta_{\rm RE} = \beta - \beta_{\rm FS}$. The rate when $I \gg 50$ mW/cm^2 is $\beta_{\rm RE} = 3.0 \times 10^{-11}$ cm^3/s. At the Doppler temperature for Cs (144 μK) and high ($I > 50$ mW/cm^2) intensities this rate yields a cross-section of $\sigma_{\rm RE}(I > 50\ {\rm mW/cm^2}) = 1.9 \times 10^{-13}$ cm^2. One of the most striking aspect of the RE rate shown in Figure 5b is that, whereas the trap depth increases with intensity (Fig. 3), the RE rate reaches a constant value at an intensity where the trap depth is still changing. Previously [13] it was suggested that as the trap depth increased, the net RE loss rate would simultaneously decrease because the energy released in RE would become less than twice the trap depth.

One interpretation of our experimental observations is that, at high intensities ($I > 50$ mW/cm^2), most of spontaneous decay which drives RE occurs at small internuclear spacing, so small that the energy released exceeds the trap depth. In this picture, the saturated (flat) intensity dependence in Figure 5b suggests that most RE happens at distances where the potential has dropped in energy by more than 22–24 GHz, with the vast majority of RE-class events therefore resulting in trap loss. According to the C_3 coefficients calculated by [23], $C_3 = -1.993 \times 10^5$ cm^{-1} Å^3, and measured by [24], $C_3 = -2.022 \times 10^5$ cm^{-1} Å^3, we estimate that, in this scenario, the spontaneous emission which leads to RE would have to occur at a distance $R_{\rm RE} < 63$ Å.

Figure 6 shows the ratio of the FS collision rate to the RE collision rate as a function of intensity, $\beta_{\rm FS}/\beta_{\rm RE}$. This value was calculated in [12] to be 65:35 = 1.8

for $I = 10$ mW/cm^2, $\Delta = -1\Gamma$, and $T = 130$ μK. The value shown in Figure 5 is quite different. The measured ratio of FS changing collisions to RE collisions is $\beta_{\rm FS}(I > 20$ mW/cm$^2)/\beta_{\rm RE}(I > 20$ mW/cm$^2) = 0.58 \pm 0.03$ and is constant within the accuracy of the experiment. The difference between the theoretically calculated value of $\beta_{\rm FS}/\beta_{\rm RE}$ and that measured could be attributed to the difficulty in calculating the Franck-Condon factors for the decay back to the ground state.

4 Conclusion

We have measured the rate of FS changing collisions and RE collisions occurring in the MOT. The cross-section for FS changing collisions is $\sigma_{\rm FS}(I > 50$ mW/cm$^2) = 1.1 \times 10^{-13}$ cm^2. The cross-section for RE collisions is $\sigma_{\rm RE}(I > 50$ mW/cm$^2) = 1.9 \times 10^{-13}$ cm^2. We found that the RE collision rate suggests that the majority of the spontaneous emission which occurs during a collision and causes RE takes place at distances $R_{\rm RE} < 63$ Å. Many questions about these collisions which occur near the dissociation limit remain; most notably the role of hyperfine structure.

This work was supported by the National Science Foundation, the David and Lucile Packard Foundation and the Army Research Office. J.P. Shaffer would like to thank the Horton Foundation for financial support. We acknowledge invaluable conversations with E. Arimondo, A. Fioretti and J. Müller. We also note that during the revision of this manuscript, we learned that the PISA group has obtained further data on Cs trap loss and that their results when combined with their previous measurements of the FS rate are in very good agreement with the results presented in this paper [25].

References

1. J. Kawanaka *et al.*, Phys. Rev. A **48**, R883 (1993); N.W. Ritchie *et al.*, Phys. Rev. A **51**, R890 (1995).
2. M. Prentiss *et al.*, Opt. Lett. **13**, 452 (1988); L. Marcassa *et al.*, Phys. Rev. A **47**, R4563 (1988); J.P. Shaffer *et al.* (to be published).
3. D. Hoffman *et al.*, Phys. Rev. Lett. **63**, 961 (1992); C.D. Wallace *et al.*, Phys. Rev. Lett. **69**, 897 (1992); P. Feng *et al.*, Phys. Rev. A **47**, R3495 (1993).
4. D. Sesko *et al.*, Phys. Rev. Lett. **63**, 961 (1989).
5. C. Williams, P.S. Julienne, J. Chem. Phys. **101**, 2634 (1994); C.J. Williams *et al.*, Phys. Rev. A **53**, R1939 (1996).
6. P.S. Julienne, A.M. Smith, K. Burnett, in *Advances in Atomic, Molecular, and Optical Physics*, edited by D.R. Bates, B. Bederson (Academic Press, San Diego, 1993), Vol. 30.
7. K.-A. Suominen *et al.*, Phys. Rev. A **57**, 3724 (1998).
8. L.G. Marcassa *et al.*, J. Phys. B **29**, 3051 (1996).
9. A. Fioretti *et al.*, Phys. Rev. A **55**, R3999 (1997).
10. T. Walker, P. Feng, *Advances in Atomic, Molecular, and Optical Physics*, edited by B. Benderson, H. Walther (Academic Press, San Diego, 1997), Vol. 34.
11. E.I. Dashevskaya, Opt. Spektrosk. **46**, 423 (1979).
12. P. Julienne, J. Vigué, Phys. Rev. A **44**, 4464 (1994).
13. P.D. Lett *et al.*, J. Phys. B **28**, 65 (1995).
14. E.L. Raab *et al.*, Phys. Rev. Lett. **59**, 2631 (1987).
15. A. Cable A. *et al.*, Opt. Lett. **15**, 507 (1990).
16. J.P. Shaffer *et al.*, App. Phys. B (to be published).
17. V.I. Balykin, Opt. Commun. **33**, 31 (1990); I.I. Sobel'man, *Introduction to the Theory of Atomic Spectra* (Pergamon Press, New York, 1972).
18. The background collision crossection as written here is dominated by collisions between excited trapped ultracold atoms and hot ground state atoms. The reason for this is that the background collisions are dominated by collisions where one of the atoms is in the excited state because the resonant dipole interaction gives a cross-section which dominates all other processes [19]. The background collisions between trapped and hot atoms have to be averaged over the probability that one of the atoms is excited. Most of the hot atoms passing through the trap are Doppler shifted too far out of resonance with the laser fields for the probability of an excited background ground state trapped atom collision to be substantial.
19. E.I. Dashevaskaya *et al.*, Can. J. Phys. **47**, 1237 (1969); L. Krause, Appl. Opt. **5**, 1375 (1966).
20. The rms velocity is $v_{\rm rms} = \sqrt{8k_{\rm B}T/\pi m}$; see F. Reif, *Fundamentals of Statistical and Thermal Physics* (McGraw-Hill, New York, 1965).
21. C.S. Adams, E. Riis, Prog. Quant. Elect. **21**, 1 (1997).
22. A. Gallagher, D.E. Pritchard, Phys. Rev. Lett. **63**, 957 (1989).
23. M. Marinescu, A. Dalgarno, Phys. Rev. A **52**, 311 (1995).
24. K. Jones *et al.*, Europhys. Lett. **35**, 85 (1996).
25. A. Fioretti, Personal communication, March 1999.